13th International Symposium on Particle Image Velocimetry – ISPIV 2019
Munich, Germany, July 22-24, 2019

Multi-angular recording technique on a single camera for 3D measurements in fluid mechanics

Corine Lacour, Petra Daher and Bertrand Lecordier*

Normandie University, UNIROUEN, INSA ROUEN, CNRS, CORIA, 76000 Rouen, France

* bertrand.lecordier@coria.fr

Abstract

The three-dimensional measurement approaches are used more and more frequently in fluid mechanics, whether to measure flow velocity, to detect of surface location (vibration, liquid gas interface) or to obtain a scalar field (flame emission, LIF 3D, density...). In practice, they consist mainly in observing the area of interest from different angles of view before carrying out a volume reconstruction, the number of viewing angles often having to be greater than three. These 3D approches lead to a significant complexity in the optical arrangement and induces significant costs (cameras, lenses ...).
For surface reconstruction, it is possible in some cases to consider approaches where several angles of view are recorded on the same detector. In this work, this kind of approach is considered by using an optical device placed in front of a single camera to record four angles of observation on the same sensor. For surface localisation, using the technique of "speckles", this recording approach is validated from four different examples. The accuracy of surface localisation is assessed and potentials of our approach for investigating fluid/structure interactions are demonstrated.

1 Introduction

The three-dimensional approaches in fluid mechanics are used increasingly over the last 10 years, whether to measure instantaneous 3D velocity fields (Elsinga et al. (2006)), surface deformations (vibration, liquid-gas interface) (Gomit (2013)) or 3D scalar fields (flame emission, LIF 3d...) (Upton et al. (2011)). They generally consist in observing the physical quantity to be studied from different angles of view, and then reconstruct its 3D distribution using entirely numerical techniques. If this type of multi-angular approach is used for decades in areas such as the health (3D scanner, MRI), their applications to fluid mechanics are much more recent. This can be explained partly by the fact that in fluid mechanics, the observed quantity is continuously changing with time and so requires simultaneous recordings of the different angles of view rather than sequential acquisitions. In practice, the number of angles of observation is often less than 6 and then it is complex to reconstruct 3D from a limited number of views. When the spatial resolution is not a key point for the measurement, it is then possible to consider the approaches from several angles of view recorded on the same sensor (Pan et al. (2017)). For this, an optical device is placed in front of the lens to split the different viewing angles onto distinct areas of the same sensor. Apart from reducing the cost of the recording device, this also makes it possible to use a specific camera (intensified, high-speed detector...) without multiplying the number.

In the present work, the recording on the same high-speed detector (Phantom V10 2400 x 1800 pixels 10 bits at 1000 fr/s) of a set of angular views of a scene through a mirror arrangement is proposed. From this optical arrangement, 4 fully dissociated angular views are recorded on the camera sensor. For each recording direction, two mirrors adjust the viewing angle and compensate for differences in optical path in order to ensure a sharped image on the detector. In order to study 3D object localisation, the "speckled" method, namely blackening

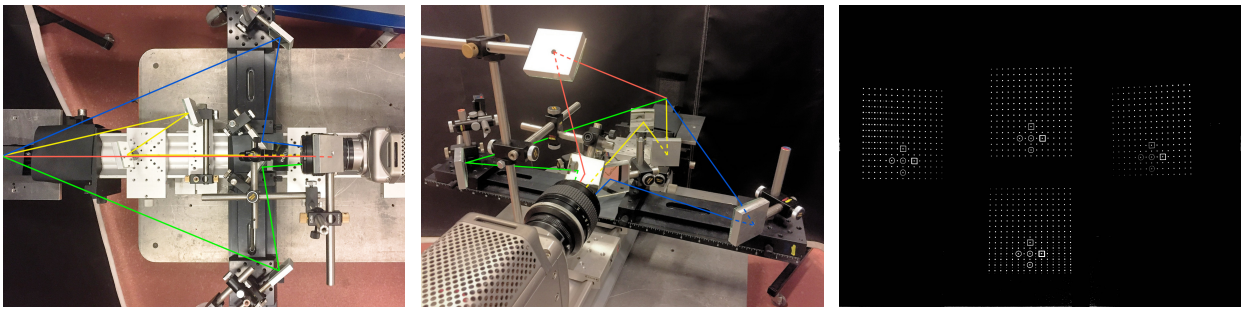

Figure 1: Multi-angle recording device and image of a calibrated grid

surfaces and painting white dots in low density has been adopted. Those points on the surface are used during the 3D reconstruction of the surface. In order to validate this approach, in this work, 4 examples of application allowing to assess the accuracy of the localisation of the surface, but also to evaluate the potential of this single-camera device to study the vibration of the surface of the surface are proposed.
In this paper, we will start with the presentation of the optical arrangement and the analysis method for the reconstruction of the surface, then we will present 4 examples of 3D surface reconstruction applications. Two calibration experiments will be performed for accuracy assessment from a translating flat plate and four calibrated cylinders. Then, the surface reconstruction technique will be illustrated by tracking the deformation of a flexible plate oscillating in a turbulent jet and the rotating motion of a fan blade.

2 Experimental set-up and data-processing

First, the optical arrangement allowing the multi-angle recording on a single detector will be presented. In a second part, the treatment performed on the images for the volume calibration and the surface reconstruction will be detailled.

2.1 Optical arrangement

In the present work, the recording on the same high-speed detector (Phantom V10 2400 x 1800 pixels 10 bits at 1000 fr/s) of a set of angular views of a scene through a mirror arrangement is proposed. The entire separation and recording devices is shown in Figure 1, where the different optical paths of imaging are schematized by color lines. The optical arrangement is placed in front of the camera, mounted with a Nikon lens of 85 mm ($f/d_{max} = 1.4$).

This optical splitting system records on the sensor, 4 angular views fully dissociated. For each recording direction, a set of two mirrors adjusts the viewing angle and compensate for optical path differences to ensure sharpness of the image on the detector. In the figure 1 on the right is presented the image recorded under the 4 observation angles of a calibration plane located at the center of the investigation domain. On these 4 views, the differences of trapezoidal deformation of the regular pattern show the effect of the recording under the different angles of observation.

2.2 Data processing for 3D surface reconstruction

To localise the points of the speckles painted on the surfaces in 3D, several steps are necessary. First, the camera calibration step is performed by moving through out the entire investigation domain with a calibrated grid fixed on a motorised translation. For each of the positions of the grid along the z axis, the location of the grid points is extracted with a sub-pixel accuracy using a pattern correlation technique. The different planes are used to determine the parameters of the polynomial model for the cameras. The order of the model can be adjusted up to 20 in all the direction and so with higher order than the Soloff model conventionally used (3, 3 and 2 respectively following x, y and z). It makes it possible to take into account the strong distortion

effects of the imagery and gives access to reconstructions on thick volumes necessary for the study of large amplitude vibration phenomena. In the present study, for the 3D calibration of the device, 21 shots are recorded and allows reconstruction over a depth of more than 50 mm (model order: 5, 5 and 3 respectively following x, y and z).
Next to the calibration step, for the reconstruction of the surface, a pre-processing of the images is carried out in order to conserve only the signal of the white dots before applying a MLOS reconstruction (Atkinson and Soria (2009)). The 3D position (x_i, y_i, z_i) of the dots p_i in the volume is then determined by a volume detection approach by thresholding and localisation of the median intensity. In order to limit the number of ghost dots, a validation step of each particle p_i is carried out by a back projection on the images to check the presence of a point of the speckle in the zone considered. The extracted dots of the surface is validated if the signal is present with a low positioning tolerance on the 4 views. In our case, this kind of very simple volume reconstruction is possible because the density of the white dots on the surfaces is relatively low. The entire procedure of volume reconstruction and extraction of the position of the points p_i has been optimised keeping between each calculation the maximum of redundant information and parallelising the codes developed at CORIA. The time for the reconstruction of a volume and extraction of the surface from 4 views ranges between 1 to 2 seconds on a latest generation of laptop. (Intel i7 2.7 Ghz - 4 cores).

3 Results and analysis

In order to validate our 3D acquisition system and the surface reconstruction process, 4 validation cases are proposed:

- Flat surface moving along the optical axis z
- Reconstruction of curved calibrated surfaces
- Flexible plate oscillating in a turbulent flow
- 3D Reconstruction of fan blades in rotation

The two first one are used to evaluate the accuracy of our surface reconstruction technique whereas that the two last one have been proposed to illustrate our approach in real conditions and show its potentials to track surface displacements

3.1 Flat surface moving along the optical axis z

The first experiment consists in moving a rigid plane along to the optical axis of the camera (axis z). For the reconstruction, the surface faced to the camera is blackened and speckled with small white dots. The plate is fixed on a motorised translation stage providing an accuracy in positioning better than 10 μm (Figure 2). For the experiment, the plane goes through the whlole calibration domain between $z = -45$ and $z = 15$ mm by increments of 0.5 mm. The plate is illuminated in continuous white light and the integration time of the CCD camera is set to 100 ms.

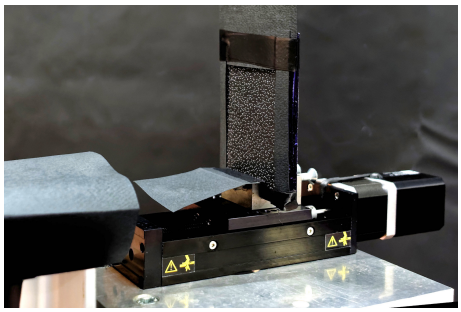

Figure 2: Device for translating the plane along the optical axis z

The extraction of the white points from the records using the procedure previously described is presented on the figure 3 (left). The color of the dots in this representation indicates the depth in the domain along the z axis. A good separation of planes with a very small dispersion in z of the reconstructed points of each individual plane location is observed. By using a 2D interpolation on a regular mesh from the extracted dots randomly distributed over the surface, the positioning of the planes in space is measured with a great precision (figure 3) In order to evaluate the accuracy of surface positioning in 3D, from the reconstructed volumes, the integrated intensity profiles along the x/y direction have been plotted as a function of z (figure 4).

Each profile corresponds to a volume and therefore a position of the plane in the domain of investigation. A very weakly dispersed of intensity profiles indicates a precise positioning of the intensity in the volume and thus of the reconstructed dots. For a quantitative evaluation of the positioning accuracy of the planes, from the coordinates (x_i, y_i, z_i) of the extracted points p_i in the volumes, the root-mean-square deviation of the z_i coordinate is computed. These results are reported in the figure 5 for each individual plan as a function of z. On one hand, the weakest dispersion is naturally in the center of the calibration zone, corresponding to the sharpest images and where the errors of the camera models are minimal. On the other hand, the further one moves away from this optimal central position and more the scatter of positioning of points along z increases. This is mainly due to an increase in the size of the image of the spots of the speckle and a loss of contrast on the images for unfocused planes on both outer sides of the calibration domain. However, for plane positions ranging in z from -30 to 10 mm, the dispersion is just slightly greater than 100 μm and more or less constant. This result indicates then a significant depth of field allowing to track surface positioning within a wide spatial domain compatible with investigation of object vibration.
Nevertheless, from the magnification factor and the CCD pixel size, we think that an accuracy better than 50 μm could be reached to locate the surface. We expect that the precision evaluated in this work may be slightly underestimated due to a small misalignment of the plane that tends to increase artificially the RMS ($z \cong constant$). The second aspect could be a characteristic *voxel* size of 100 μm for the reconstruction step which is certainly too large compared to the expected accuracy, even if the particle location is extracted with sub-voxel accuracy.
In future work, these two aspects will be considered in order to make an estimate of the maximum precision that we can expect with this device.

3.2 Reconstruction of curved calibrated surfaces

Figure 6: View of the 4 calibrated cylinders with speckled dots

To evaluate the accuracy of surface reconstruction by a second approach, 4 cylinders of different calibrated diameters ($R = 10.10$, 20.25, 30.30 and 35.08 mm) painted in black with speckled white dots randomly distributed have been designed (Figure 6). These cylinders were positioned successively at the center of the measuring domain and illuminated with a continuous white light as for the previous case.
The point extraction of the surface for the cylinder $R = 30.30$ mm is shown on the left part in the figure 7. Satisfactory point extraction over a large depth of field with good homogeneity in positioning of the points along the main axis of the cylinder is observed. This last point is confirmed on the right side of the figure where the lines of iso-height on the entirety of the reconstructed zone are regularly distributed and parallel whatever the z position.
The last validation of surface reconstruction from the cylinders is based on a comparison of the measured diameter with the actual diameter of the calibrated cylinders. These results are presented on the figure 8 in the X/Z plane where all the extracted points whatever its height along y are plotted and superimposed to the cross-section of the four cylinders (dotted lines). For all the cases, an excellent concordance between the measurement and the "theoretical" positioning of the surface of the calibrated cylinders is noted. For the first three cylinders, the points extracted overlap perfectly with the circle. For the largest diameter, a slight increase in dispersion is observed. It can be explained by a different speckle and in particular lower density of dots with lower contrast than for the other three cylinders (Figure 6).
For the 4 cases, the reconstruction is carried out on approximately 10 mm in depth because the points beyond these positions cannot be observed according to the four angles of view, criterion imposed in the reconstruction and the extraction spots of the speckle.

3.3 Flexible plate oscillating in a turbulent flow

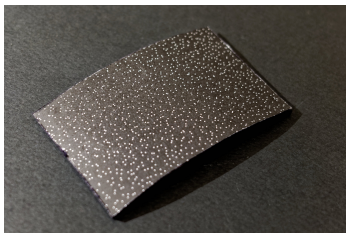

Figure 9: Flexible plate

The first application of our recording method for surface reconstruction is a flexible plate (made in rubber) oscillating in a turbulent air jet (Figure 9). The plate is fixed by one of its ends and under the effect of the impulse of the fluid on its rear face, the plate oscillates. The recordings were made by illuminating the plate with an Nd:YAG laser delivering double pulses of 30 mJ at 20 Hz. To obtain a uniform illumination on the entire surface of the plate, a diffuser has been used.
The first results for 3 instants are shown in figure 10. On the left side, the position (x_i, y_i, z_i) of the p_i points extracted from the records are plotted. These points are difficult to analyse directly, varying in position but also slightly in number over time according to the extraction criteria and the position of the plate. For a quantitative exploitation of these measurements, the surface equation $z = f(x,y)$ is extracted from to the coordinates $(x_i(z_i), y_i(z_i))$ using 2D polynomial. The results of the interpolation of the surface are shown in figure 10 (on the right). On these plots, the color indicates the plate height in z. The oscillation of the plate over time is clearly observed for the 3 times reported and the curvature of the iso-lines show high torsion of the plate under the effect of the jet of air.

To illustrate the potentials of this approach to investigate fluid/structure interactions, in the figure 11, the temporal evolution of the height of the point located at $(-10, 10)$ on the plate is reported. The flapping of the flexible plate with the flow is observed in spite of a little low sampling rate. A high acquisition rate would be necessary to get the fastest oscillations, but this result give an idea of the potential of our technique for a 3D reconstruction of surface from a single camera. After 20 seconds, the jet flow is stopped and the plate vibration completely stop with an equilibrium position at $z = -6.1$ mm. From this simple experiment, the interest of our approach to study with accuracy the unsteady movement and the deformation of a structure in interaction with a flow is clearly demonstrated.

3.4 3D Reconstruction of fan blades in rotation

For the last surface reconstruction illustration, the method has been applied to the case of a rotating fan blade (Figure 12). A computer cooling fan was placed in the observation area and rotated at a constant rotation speed (3000 rpm). The phasing of the acquisition (laser/camera) was carried out from the internal tachometer signal of the fan. In order to visualise the surface, two blades over seven were blackened and speckled with white paint and illuminated by a double pulse Nd: YAG laser.

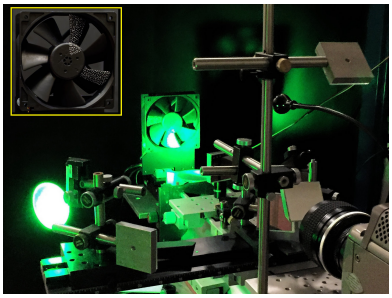

Figure 12: Fan view

The first reconstruction is presented from two perspectives on the Figure 13. To visualise the surface, a mesh obtained by triangularisation from the raw 3D points (x_i, y_i, z_i) has been created. The blades is clearly distinguished from the rotor, the connectivity surface being not reconstructed because is orientation is aligned more or less with the observation lines of sight. We can note the very good reconstruction of the profile of the blade as well as the flatness of the central rotor. In the right view, the accuracy of the 3D surface reconstruction is confirmed by the high regularity of the iso-contour lines coding the measured height. In the present work, the analysis of the double pulse recordings is not presented, but it will offer with further investigations, the instantaneous speed and acceleration of the blade. On the figure 14, an example of the reconstruction of the blade at different phase angles of the rotation is shown. In the futur works, from the speed information and the 3D surface reconstruction of the blade as a function of the phase, it will be possible to study the vibratory phenomena. For further investigations, the velocity measurement of the fluid near the fan by PIV could be associated to correlate the vibration with the air flow.

4 Conclusions and perspectives

In this article, an optical arrangement composed of eight flat mirrors has been proposed to record on a single high speed detector (1000 fr/s), 4 angular views of the same scene. This high-speed recording system was used to reconstruct and locate in 3D the surfaces of fixed or moving objects. From 4 applications (plane translation, calibrated cylinder, flexible plate and rotating fan), the potentials of this single-camera with view splitting technique for 3D surface reconstruction have been demonstrated. The translated plane and calibrated cylinders experiments have been used to asses the accuracy for the surface positioning in depth which as been evaluated at around 100 μm.

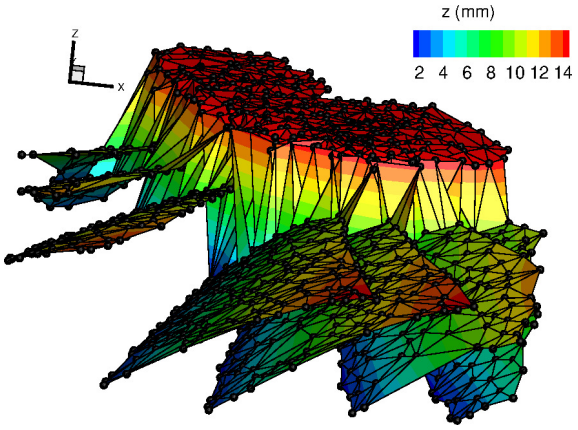

Figure 14: Superposition of the 3D reconstruction of a blade at different phases

This device is adapted for the measurement of vibration (oscillation) of surfaces with significant magnitude due to a large depth of field (40 mm). In addition, our recording system is easy to associate with the PIV technique (2D-2C, 2D-3C or 3D) and so it is particularly suitable for aero/elasticity investigation (fluid/structure interactions).
It is also possible to consider an application of this approach for PIV tomography measurements in the case where the volume sizes to be investigated are relatively small and where the spatial resolution of the velocity measurement is not necessary an issue. A validation of the device for 3D velocity measurement will be carried out in the next months.

References

Atkinson C and Soria J (2009) An efficient simultaneous reconstruction technique for tomographic particle image velocimetry. *Experiments in Fluids* 47:553–568. 10.1007/s00348-009-0728-0

Elsinga GE, Scarano F, Wieneke B, and van Oudheusden BW (2006) Tomographic particle image velocimetry. *Experiments in Fluids* V41:933–947

Gomit G (2013) *Développement de techniques de mesure de surfaces libres par moyens optiques : application à l'analyse de l'écoulement généré par un modèle de bateau en bassin des carènes*. Ph.D. thesis. Ecole doctorale : Sciences et ingénierie en matériaux, mécanique, énergétique et aéronautique - SIMMEA (Poitiers)

Pan B, Yu L, and Zhang Q (2017) Review of single-camera stereo-digital image correlation techniques for full-field 3d shape and deformation measurement. *Science China Technological Sciences*

Upton T, Verhoeven D, and Hudgins D (2011) High-resolution computed tomography of a turbulent reacting flow. *Experiments in Fluids* 50:125–134

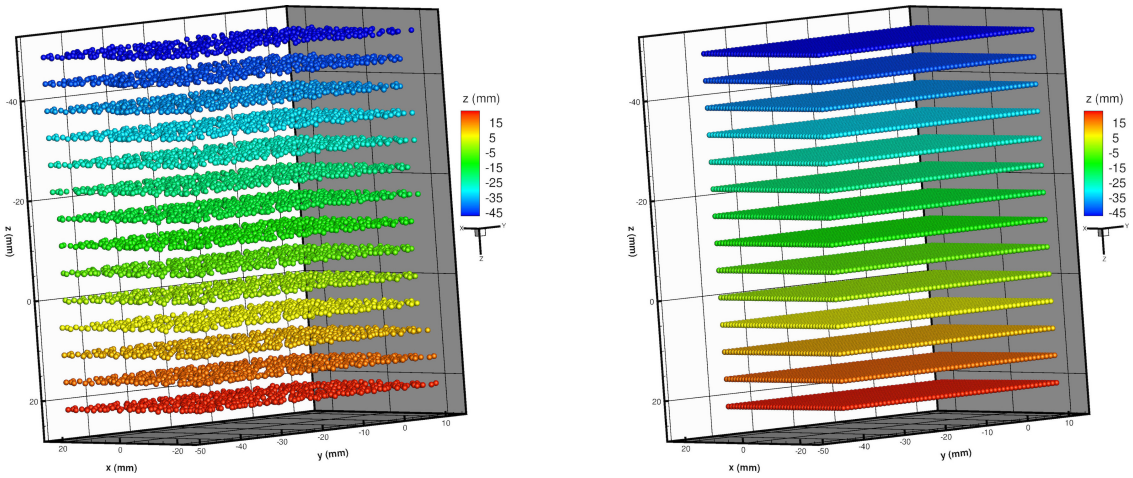

Figure 3: Reconstruction of the planes (left) and interpolation on a regular mesh (right)

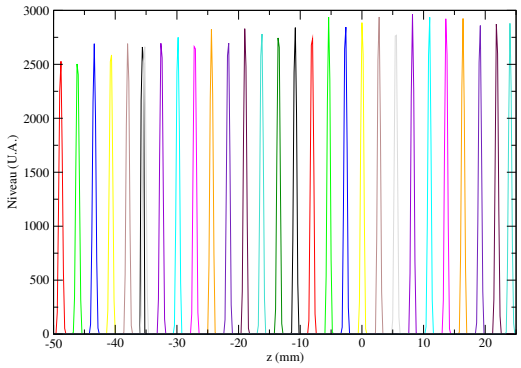

Figure 4: Intensity profiles of the reconstructed volume projection along the x/y directions

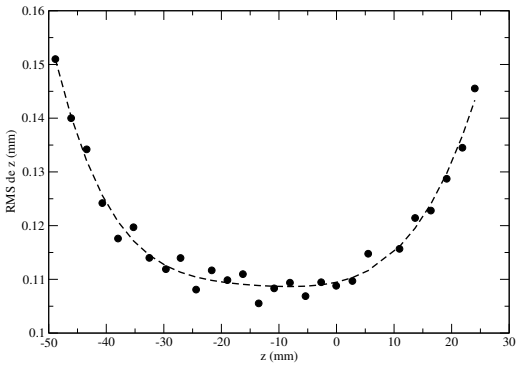

Figure 5: Dispersion of the z positioning of the reconstructed dots for the different plans

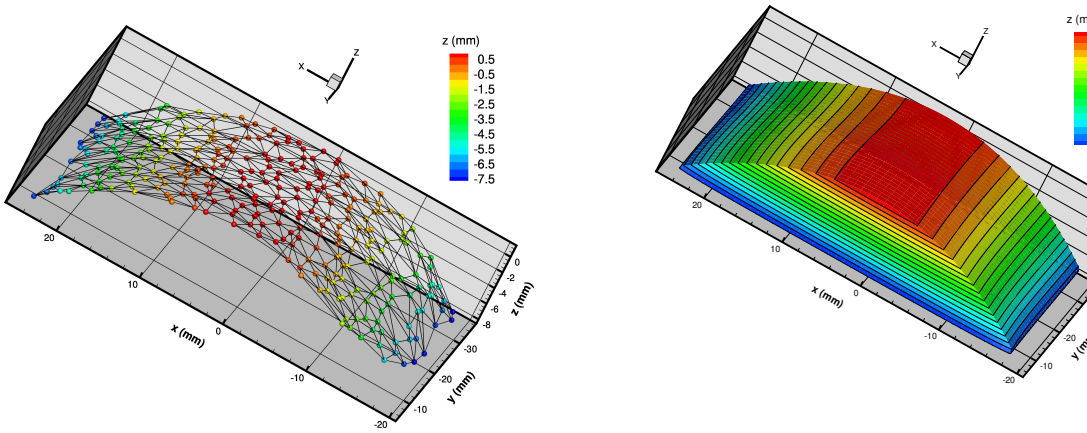

Figure 7: 3D Extraction of the white dots for the cylinder ($R = 30.30mm$) (left) and polynomial reconstruction of the surface (right)

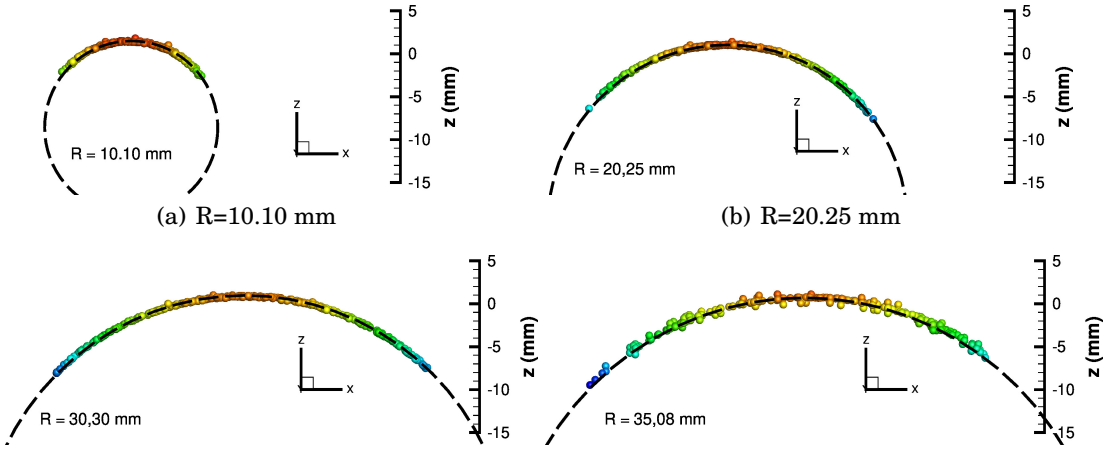

(a) R=10.10 mm (b) R=20.25 mm

(c) R=30.30 mm (d) R=35.08 mm

Figure 8: Comparison in the X / Z plane of the 3D extraction of the white surface dots compared to the calibrated cylinders

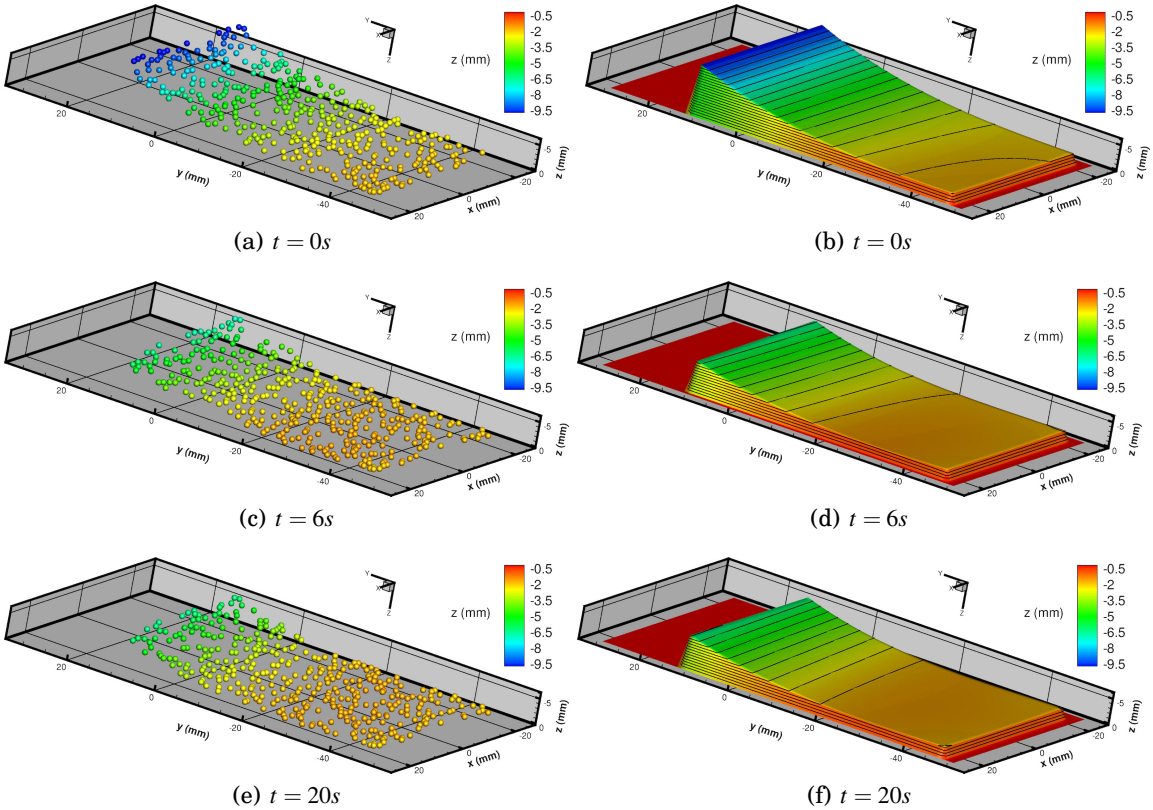

(a) $t = 0s$ (b) $t = 0s$

(c) $t = 6s$ (d) $t = 6s$

(e) $t = 20s$ (f) $t = 20s$

Figure 10: Extraction of the points of the plate for 3 different times (gauche) and polynomial reconstruction of the surface (droite)

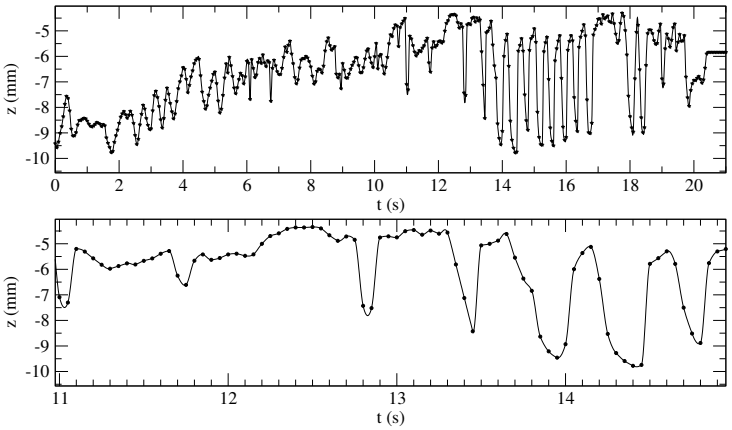

Figure 11: Temporal evolution of the point of the plate located at (-10,10)

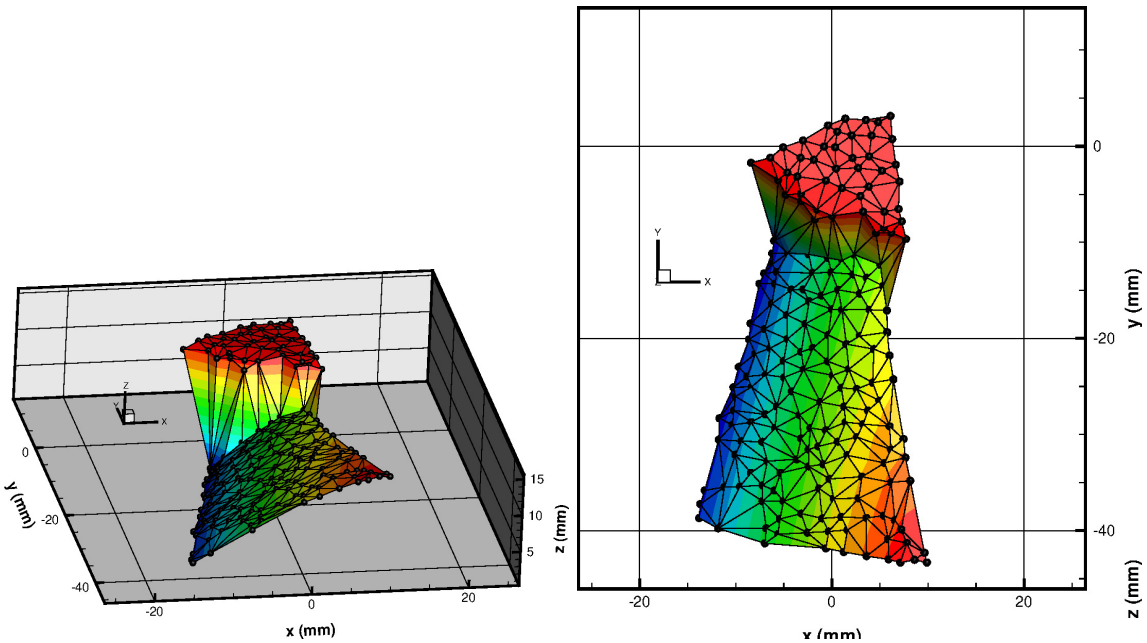

Figure 13: Example of 3D reconstruction of a rotating fan blade (3000 tr/min)